Journal of Renewable Materials

Tech Science Press

DOI: 10.32604/jrm.2021.014695

ARTICLE

Preparation and Characterization of Potassium Monopersulfate/Ethyl Cellulose Microcapsules and Their Sustained Release Performance

Qiaoguang Li[1], Xuming Yan[1], Jialong Chen[1], Xugang Shu[1,*], Puyou Jia[2,*] and Xiangjun Liang[3]

[1]School of Chemistry and Chemical Engineering, Zhongkai University of Agriculture and Engineering, Guangzhou, 510225, China

[2]Institute of Chemical Industry of Forest Products, Chinese Academy of Forestry, Nanjing, 210042, China

[3]Guangzhou Ansai Chemical Industry Co., Ltd., Guangzhou, 510225, China

[*]Corresponding Authors: Xugang Shu. Email: xgshu@21cn.com; Puyou Jia. Email: jiapuyou@icifp.cn

Received: 20 October 2020 Accepted: 03 December 2020

ABSTRACT

Environmental cleaning is an important aspect of bacteria control. Ethyl cellulose microcapsules containing potassium monopersulfate (PMCM) were prepared by emulsified solvent diffusion method. The chemical structure and microstructure of the obtained PMCM was characterized by methods of Fourier transform infrared spectroscopy (FT-IR), optical microscopy, scanning electron microscopy and X-ACT energy dispersive X-ray spectroscopy. The SEM micrographs of the PMCM containing 21.6% of C, 46.8% of O, 10.7% of S and 19.4% of K was relatively smooth. Thermal stability, sustained release performance, and antimicrobial activity of PMCM were investigated. The results showed that the drug loading and encapsulation efficiency of PMCM were 30.3% and 42.6% respectively. Potassium monopersulfate was fully released after 8 h, following a Fickian diffusion mechanism. Results showed that the microcapsules prepared with a high concentration of potassium monopersulfate solution showed a good antimicrobial effect. The microcapsule wall of the resulting PMCM increased with increasing ethyl cellulose content and had high thermal stability from the data of 69% residue rate. The excellent thermal stability and high sustained release performance of PMCM showed high application value.

KEYWORDS

Potassium monopersulfate; cellulose microcapsules; sustained release performance; preparation; characterization

1 Introduction

The inorganic peroxide, potassium monopersulfate, is a strong oxidizer. As a highly effective oxidative disinfectant, it can kill many microorganisms including bacteria, spores, viruses, fungi and so on [1]. However, the decomposition temperature of potassium monopersulfate is low and its activity is not stable long term in water, which wastes resources [2]. In such situations, microencapsulation has been used to develop a dosage form capable of the controlled release of agrochemicals and other biologically active agents such as pharmaceuticals, essential oils, and pesticides with beneficial effects [3–7]. Microcapsules are tiny particles of spherical or irregular shape containing active ingredients in its core and a polymeric shell of synthetic or natural material prepared by physical or chemical techniques [8,9]. The polymeric shell of the microcapsules can be made from synthetic polymers such as polyurea, epoxy resin, urea-formaldehyde resin [10–13] but these may be toxic to human being and the environment [14].

Consequently, researchers have recently focused on abundant, renewable, natural materials including starch, cellulose, and chitosan [15–19].

Ethyl cellulose is a non-toxic, natural material of low cost that easily degrades [20,21]. It has been extensively studied as a microencapsulating material for 5-flurouracil, aceclofenac, and diclofenac sodium in controlled release applications [22–25]. However, it has not yet been explored for encapsulating potassium monopersulfate, which is more efficacious against many infectious microorganisms such as viruses and bacteria than sodium hypochlorite (NaClO). Additionally, NaClO is problematic for reasons such as corrosion of equipment, generation of irritating chlorine gas, and complicated management of concentrations. Alteration of any independent variable factor such as core loading, core-wall ratio may affect the final microcapsule characteristics and release kinetics [26,27].

In this work, potassium monopersulfate/ethyl cellulose microcapsules (PMCM) were prepared (Fig. 1) and a series of tests were carried out to study its chemical structure, thermal properties, drug loading, encapsulation efficiency, as well as sustained-release and bacteriostatic performance.

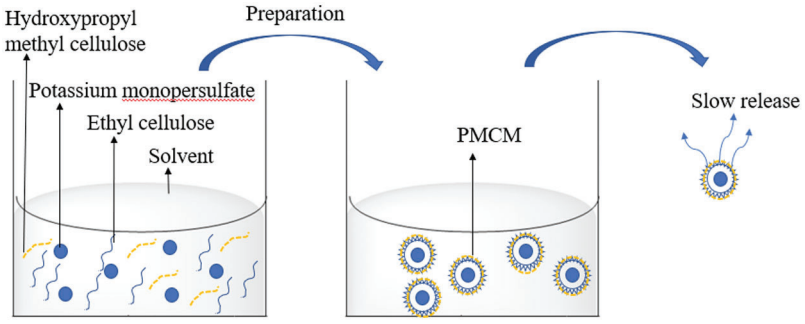

Figure 1: Ethyl cellulose microencapsulation containing potassium monopersulfate

2 Materials and Methods

2.1 Materials

Ethyl cellulose, absolute ethanol, hydroxypropyl methyl cellulose, and potassium monopersulfate were supplied by Aladdin Chemical Reagent Co. Ltd. Nutritional agar and broth medium were obtained from Beijing Solebo Technology Co., Ltd. All chemicals were used without further purification.

2.2 Synthesis of PMCM

Potassium monopersulfate (1 g) was dissolved in water (50 mL). Hydroxypropyl methyl cellulose (0.4 g) was added to this aqueous solution under continuous stirring. Separately, ethyl cellulose (1 g) was dissolved in absolute ethanol (50 mL) under continuous stirring at 60°C to form an organic solution. After the cooling to below 30°C, the organic solution was slowly added dropwise to the aqueous solution under stirring. PMCM were obtained from mixture after filtration and solvent evaporation. The core: wall ratio was determined as the mass ratio of potassium monopersulfate to ethyl cellulose.

2.3 Characterizations and Measurements

FT-IR: Fourier transform infrared (FT-IR) spectroscopy was carried out on a Thermo Scientific Nicolet IS10 spectrometer (Nicolet, USA) by ATR (attenuated total reflectance). The spectra were recorded over the range 4000–600 cm^{-1} at 4 cm^{-1} resolution and averaged over 16 scans per sample.

TG: The thermal stability of the samples was determined using a TG209F1 thermogravimetric analyzer (Netzsch, Germany). The samples were heated from 25°C to 800°C at a rate of 10 °C min^{-1} under a nitrogen atmosphere.

Optical microscopy: The shape and morphology of the PMCM were evaluated by an Olympus SX optical microscope (Japan) equipped with a Canon Powershot SX40 digital camera.

SEM: The PMCM were coated with gold. Then morphology of the PMCM was examined using a QUANTA 200 (FEI, Holland) scanning electron microscope at a voltage of 10 kV.

EDS: The elemental composition of the PMCM was performed using X-ACT energy dispersive X-ray spectroscopy (Oxford, England).

Standard curve of Potassium monopersulfate: Linear regression of the solution concentration (C) and absorbance (A) of potassium monopersulfate standard solutions of different concentrations at λ = 192 nm was performed by a UV-2550 UV-Vis spectrophotometer. The standard curvilinear equation is as follows: $A = 0.68173C+0.03847$, $R^2 = 0.99213$

2.3.1 Determination of Encapsulation Efficiency and Drug Loading of PMCM

Drug-loaded microcapsules (m_1) were transferred to a 50 mL volumetric flask, and mixed with deionized water. The volumetric flask was placed under ultrasound treatment for 40 minutes below 30°C. After filtration, this absorbance of the solution was measured by UV spectrophotometry, and the mass concentration of potassium monopersulfate was calculated. The encapsulation efficiency (*EE*) and loading content (*LC*) were obtained by the following Eqs. (1) and (2) [28,29]:

$$\mathrm{LC} = \frac{m_2}{m_1} \times 100\% \tag{1}$$

$$\mathrm{EE} = \frac{m_2}{m_3} \times 100\% \tag{2}$$

where m_1 is the mass of microcapsules (mg), m_2 is the mass of potassium monopersulfate in microcapsules (mg), m_3 is the mass of potassium monopersulfate in preparation microcapsules (mg).

2.3.2 Determination of Sustained Release Properties of PMCM

The drug-loaded microcapsules (0.15 g) were placed in a conical flask filled with 100 ml of deionized water in a water bath oscillator at 25°C. At intervals of time, 3 ml of the sample solution was removed and the concentration of potassium monopersulfate was determined by UV. Then an equal volume of the sustained release medium was added to the conical flask to replace the withdrawn sample. Then the dynamics curve of the release quantity fraction - time was plotted.

2.3.3 Antibacterial Effect of PMCM

The experiment was divided into three steps: Cultivating strains, selecting appropriate dilution concentration of strains, and testing the bacteriostasis effect according to the literature [26,27]. The samples corresponding to the PMCM microspheres, for example, 0.1 g drug-free microcapsules, 0.1 g potassium monopersulfate microcapsules, and no microcapsules, were added to the hole for allowing to naturally release potassium monopersulfate after 24 h at 37°C, respectively. The diameter of inhibition zone was measured via a cross intersection method. The larger the circle without bacteria is, the stronger the antibacterial activity is, which means that the bacteria cannot easily grow in the presence of potassium persulfate.

3 Results and Discussion

3.1 Effect of the Ratio of Core-Wall on Encapsulation Efficiency and Drug Loading

From Tab. 1, with the decrease in the ratio of core-wall, the content of ethyl cellulose increaseed, thus the drug loading of microcapsules was relatively reduced [28]. The drug loading of microcapsules was reduced from 37.6% to 26.7%. For the encapsulation efficiency, potassium monopersulfate was more likely to be encapsulated with the increase in ethyl cellulose concentration. Therefore, the encapsulation efficiency increased from 26.1%, 42.6% to 59.4% respectively [29]. Previous studies in this area are summarized in Tab. 2.

Table 1: Effect of the ratio of core-wall on drug loading and encapsulation efficiency

Core-wall ratio	Encapsulation efficiency/%	Drug loading/%
1:0.5	26.1	37.6
1:1	42.6	30.3
1:2	59.4	26.7

Table 2: Comparisons of encapsulation efficiency of microcapsules

Raw material	Core	Encapsulation efficiency/%	Ref(s).
ethyl cellulose	**potassium monopersulfate**	**59.4**	**This work**
ethyl cellulose	Salbutamol sulphate	46.5	[20]
ethyl cellulose	myristic acid	62.0	[23]
ethyl cellulose	propranolol hydrochloride	77.7	[25]
ethyl cellulose	plant oils	70.0	[30]
ethyl cellulose	linseed oil	64.4	[31]

3.2 Sustained-Release Properties of PMCM

As shown in Fig. 2, the release amount of the drug in sustained-release PMCM gradually increased with increasing time. The sustained release curve showed a quick release trend at first, with a slower release thereafter. Significant “sudden release” of more than 25% release rate was observed at about 1 h. For example, when the core-wall ratio was 1:0.5, the initial reached rate reaches 46%. The rapid release may be of the free potassium monopersulfate from microcapsule surface.

With the increase in core-wall ratio, the release rate of microcapsules increasesed. The more the amount of encapsulated potassium monopersulfate, the thinner the wall thickness of microcapsules. The sustained release performance is closely related to core-wall ratio. The wall thickness of the microcapsules relates to the diffusion path of potassium monopersulfate from the inside of the microcapsules to the outside medium [28]. Hence, more thickness of microcapsules will show more release time. However, if the core-wall ratio is small, the microcapsule will be too dense and too thick, and thus, it is difficult for the potassium monopersulfate to be released to the outside. When the core-wall ratio was 1:2, the final cumulative release rate was only 47%. A large amount of the drug was released from the microcapsule within a short time to eliminate bacteria and the slow sustained release of the drug could maintain effective activity for a long time. Considering comprehensively, the core-wall ratio of 1:1 was selected to prepared microcapsules with good sustained-release performance.

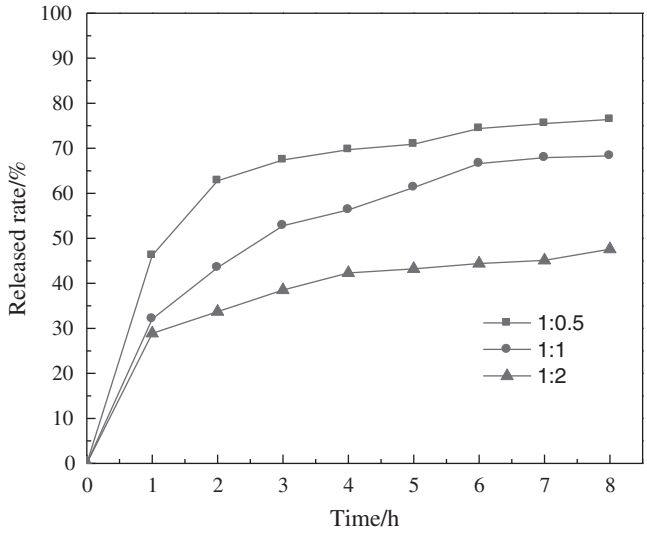

Figure 2: Effect of core-wall ratio on sustained-release properties of PMCM

3.3 Kinetics Study of PMCM

To further study the sustained release mechanism, the data of sustained release of potassium monopersulfate from PMCM were fitted to the Higuchi model and Korsmeryer-Pappas model using the data of sustained-release performance of microcapsules with the core-wall ratio of 1:1. The corresponding Eqs. (3) and (4) are as follows [32,33]:

Higuchi model:

$$Q_t = Kt^{1/2} \tag{3}$$

Korsmeyer-Peppas model:

$$Q_t = Kt^n \tag{4}$$

where Q_t represents the cumulative release percentage of potassium monopersulfate at t time, K is the release constant of potassium monopersulfate, and n represents the diffusion constant of potassium monopersulfate. The results are shown in Tab. 3, which are consistent with the Korsmeryer-Pappas kinetic equation. The value of diffusion coefficient n was 0.3715. As n is below 0.45, it means that the sustained release of potassium monopersulfate is controlled by a Fickian diffusion mechanism.

Table 3: Fitting results for drug release curves of PMCM

Kinetic model	Fitting equation	R^2
Higuchi	$Q = 0.2024t^{1/2}+0.1485$	0.966
Korsmeyer-Peppas	$lnQ = 0.3715ln(t)-1.0983$	0.983

3.4 Effect on Antimicrobial Activity of PMCM

As shown in Figs. 3a–3b, staphylococcus aureus colonies were very dense around the round hole with no PMCM and drug-free PMCM, suggesting that ethyl cellulose had no bacteriostatic performance. Fig. 3c proved that microcapsule with 20% concentration of potassium monopersulfate had a remarkable bacteriostasis performance from the result of a large bacteriostasis circle. This indicates the strong bactericidal ability of potassium monopersulfate and the potential slow-release performance of PMCM.

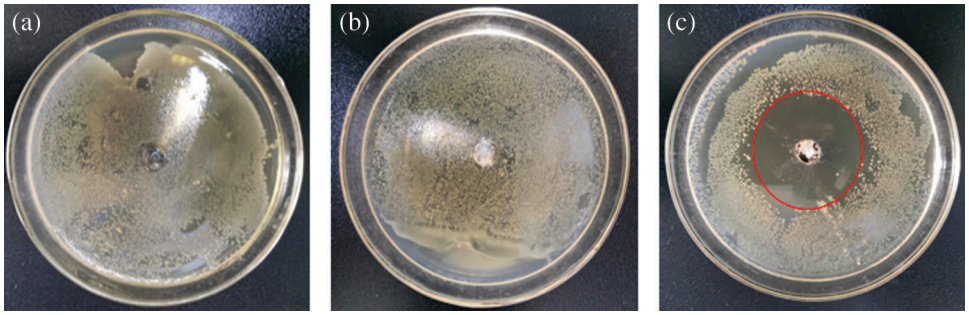

Figure 3: Effect on antimicrobial activity of PMCM; a: no PMCM, b: 0.1 g drug-free PMCM, c: 0.1 g PMCM

3.5 FT-IR Analysis

FT-IR spectra of the ethyl cellulose (a), potassium monopersulfate (b), and PMCM (c) are shown in Fig. 4 [34–36]. In a spectrum, the absorption band at about 3500 cm^{-1} corresponds to the OH stretching vibration peak. The absorption peak observed at 2871 cm^{-1} is due to the presence of CH_3 symmetrical stretching vibration peak. In b spectrum, the peak at about 1000 cm^{-1} represents the characteristics of S-O, and 3214 cm^{-1} corresponds to the OH stretching in core of potassium monopersulfate. In c spectrum, at 1000 cm^{-1}, 2871 cm^{-1}, 3214 cm^{-1} and 3500 cm^{-1} are the characteristics peaks of the S-O, CH_3 and OH. The same characteristic peaks for different functional groups present in core of potassium monopersulfate and in PMCM confirmed the formation of ethyl cellulose (shell) and potassium monopersulfate (core) present in the microcapsules.

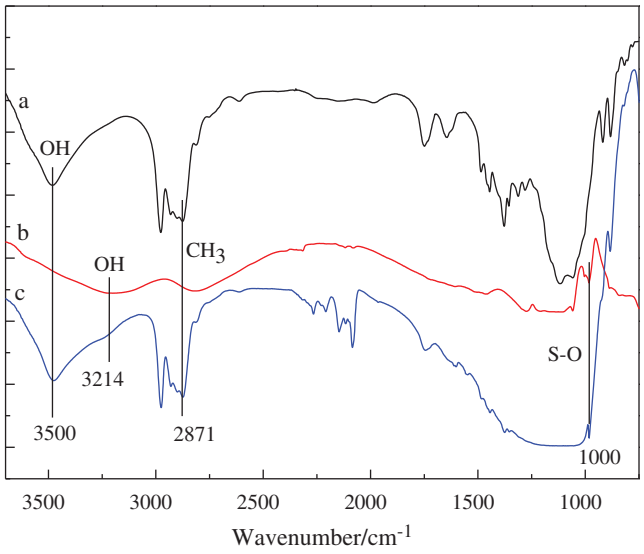

Figure 4: FT-IR characterization of PMCM; a: Ethyl cellulose, b: Potassium monopersulfate, c: PMCM

3.6 Optical Micrographs and SEM Analysis

The optical micrographs of PMCM are shown in Fig. 5, in order to illustrate PMCM with different microcapsule walls [37–39]. Clearly, the microcapsules prepared in this work showed consistent results. The transparency of PMCM became poor from Figs. 5a–5c, because of the increase in the microcapsule wall thickness of PMCM.

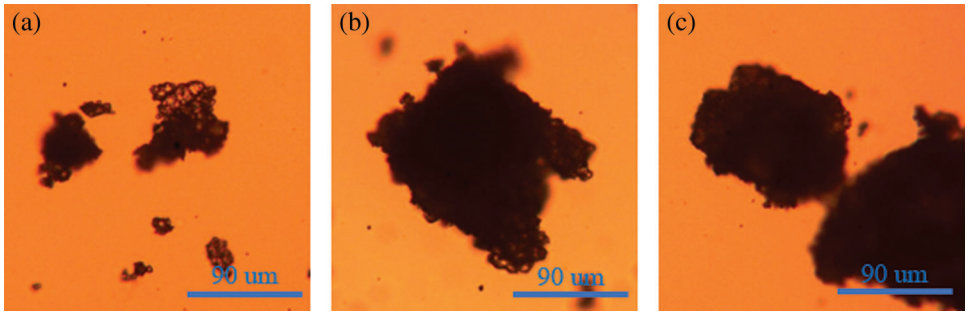

Figure 5: Optical micrographs of PMCM; a: The PMCM with core-wall ratio of 1:0.5, b: The PMCM with core-wall ratio of 1:1, c: The PMCM with core-wall ratio of 1:2

Fig. 6 shows the SEM micrographs to reveal the surface details of PMCM [40,41]. The external surface of the microcapsules was relatively smooth and without aggregation in Figs. 6a and 6b from these micrographs. As seen in Fig. 6c, the PMCM undergoesaggregation due to an excess of ethyl cellulose. However, PMCM in Fig. 6b has relatively homogeneous size. The results of optical micrographs and SEM micrographs of PMCM are consistent with the result of sustained-release properties.

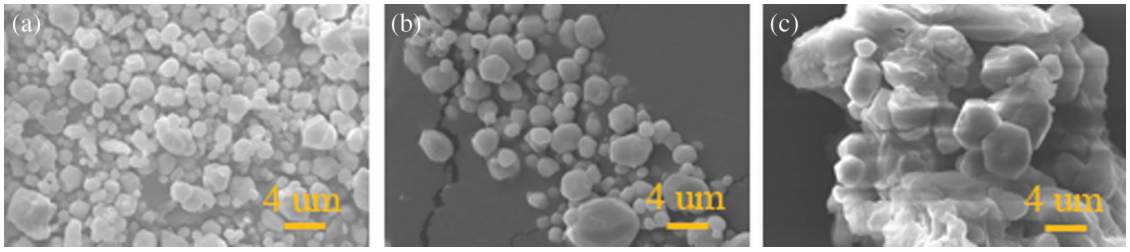

Figure 6: SEM micrographs of PMCM; a: The PMCM with core-wall ratio of 1:0.5, b: The PMCM with core-wall ratio of 1:1, c: The PMCM with core-wall ratio of 1:2

3.7 EDS analysis

The EDS spectra and elemental composition of PMCM are presented in Figs. 7 and 8. These showed that PMCM has C and O elements from ethyl cellulose and S and K elements from potassium monopersulfate. The contents of C, O, S and K elements were 21.6%, 46.8%, 10.7% and 19.4%, respectively.

3.8 Thermal Properties

As shown in Figs. 9 and 10, thermal degradation of ethyl cellulose (a), potassium monopersulfate (b), PMCM (c) was investigated by TG [42–44]. In DTG curve of b, a relatively small maximum weight loss rate at nearly 120°C occurred due to the decomposition of potassium monopersulfate with corresponding fast decomposition in TG curve at this temperature. In TG and DTG curves of c, 5% mass loss temperature and the maximum weight loss rate temperature were at 200°C and 220°C, respectively. The residue rate was 69% at 500°C. Potassium monopersulfate had the lowest decomposition temperature and ethyl cellulose had the least residue rate. Results proved that ethyl cellulose as wall material of microcapsules showed good thermal stability and high temperature resistance. These data suggested that PMCM with excellent thermal stability can be used as sustained-release microcapsules for high temperature applications [45].

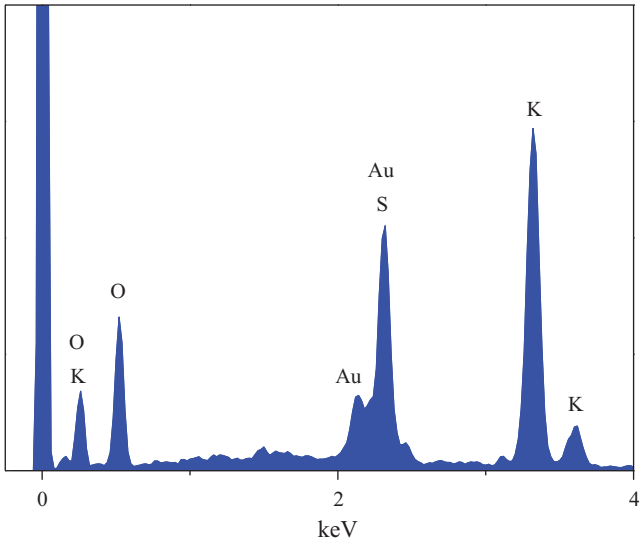

Figure 7: EDS spectra of PMCM

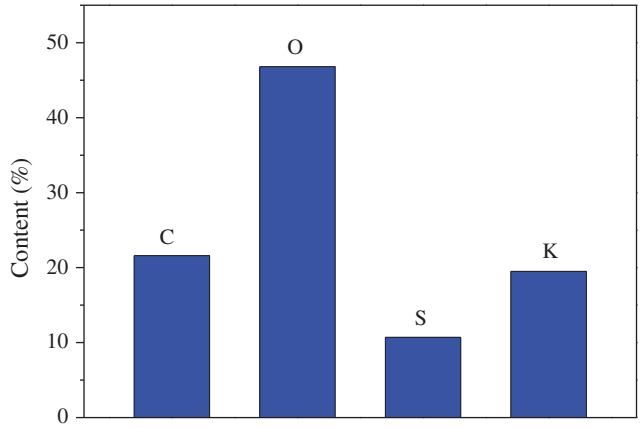

Figure 8: Element composition of PMCM

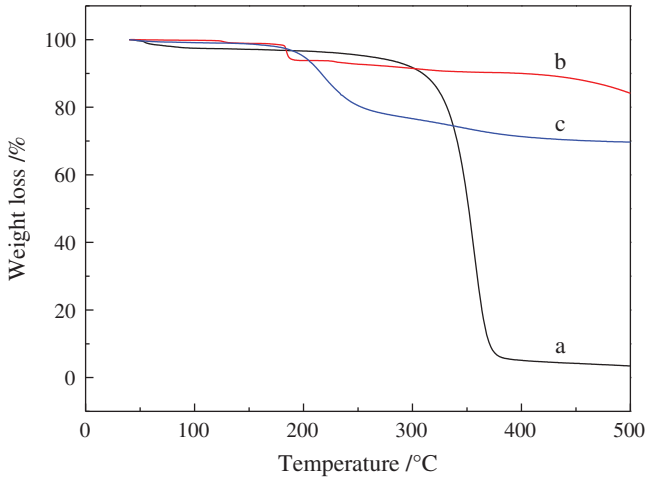

Figure 9: The TG curves of a: Ethyl cellulose, b: Potassium monopersulfate, c: PMCM

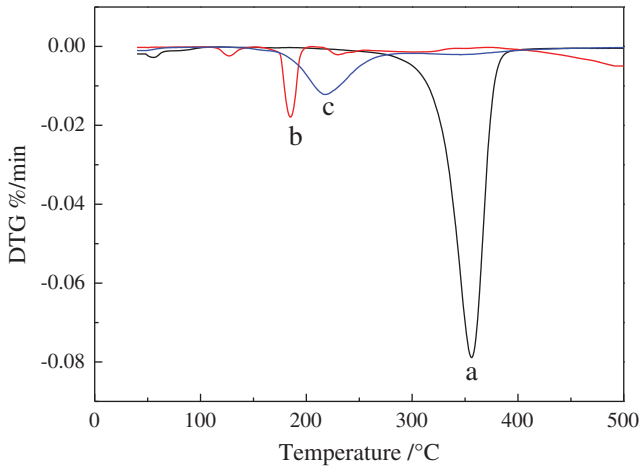

Figure 10: The DTG curves of a: Ethyl cellulose, b: Potassium monopersulfate, c: PMCM

4 Conclusions

In summary, PMCM containing potassium monopersulfate was successfully prepared and characterized. PMCM with 30.3% drug loading and 42.6% encapsulation efficiency and exhibited excellent thermal stability and good antimicrobial effect after drug release. It was found concluded that different core-wall ratios influenced the variation in drug loading as well as entrapment efficiency, and the drug release behavior. Therefore, there is great potential for the development of renewable materials (PMCM) that ensure the appropriate drug load and sustained release in industrial applications. These results may promote the prospective application of ethyl cellulose microcapsules as a suitable sustained release drug delivery system.

Funding Statement: The authors express their gratitude for the financial support From the Open Fund Project of Key Lab. of Biomass Energy and Material, Jiangsu Province (JSBEM201907), the Ordinary University Young Innovative Talents Project of Guangdong Province (2018KQNCX119).

Conflicts of Interest: The authors declare that they have no conflicts of interest to report regarding the present study.

References

1. Jin, B., Niu, J., Dai, J., Li, N., Zhou, P. et al. (2018). New insights into the enhancement of biochemical degradation potential from waste activated sludge with low organic content by Potassium Monopersulfate treatment. *Bioresource Technology, 265,* 8–16. DOI 10.1016/j.biortech.2018.05.032.
2. Liu, K., Lu, J., Ji, Y. (2015). Formation of brominated disinfection by-products and bromate in cobalt catalyzed peroxymonosulfate oxidation of phenol. *Water Research, 84,* 1–7. DOI 10.1016/j.watres.2015.07.015.
3. Ayad, M. M., Salahuddin, N. A., Torad, N. L., El-Nasr, A. A. (2016). pH-Responsive sulphonated mesoporous silica: A comparative drug release study. *RSC Advances, 6(63),* 57929–57940. DOI 10.1039/C6RA07022A.
4. El Mourabit, S., Guillot, M., Toquer, G., Cambedouzou, J., Goettmann, F. et al. (2012). Stability of mesoporous silica under acidic conditions. *RSC Advances, 2(29),* 10916–10924. DOI 10.1039/c2ra21569a.
5. Mamaeva, V., Sahlgren, C., Lindén, M. (2013). Mesoporous silica nanoparticles in medicine—Recent advances. *Advanced Drug Delivery Reviews, 65(5),* 689–702. DOI 10.1016/j.addr.2012.07.018.
6. Tang, F., Li, L., Chen, D. (2012). Mesoporous silica nanoparticles: Synthesis, biocompatibility and drug delivery. *Advanced Materials, 24(12),* 1504–1534. DOI 10.1002/adma.201104763.
7. Chen, H., Lin, Y., Zhou, H., Zhou, X. Gong, S. et al. (2016). Synthesis and characterization of chlorpyrifos/copper (II) schiff base mesoporous silica with pH sensitivity for pesticide sustained release. *Journal of Agricultural and Food Chemistry, 64(43),* 8095–8102. DOI 10.1021/acs.jafc.6b03262.

8. Meng, F., Wang, S., Liu, H., Xu, X., Ma, H. (2017). Microencapsulation of oxalic acid (OA) via coacervation induced by polydimethylsiloxane (PDMS) for the sustained release performance. *Materials & Design, 116,* 31–41. DOI 10.1016/j.matdes.2016.11.031.
9. Nedovic, V., Kalusevic, A., Manojlovic, V., Levic, S., Bugarski, B. (2011). An overview of encapsulation technologies for food applications. *Procedia Food Science, 1,* 1806–1815. DOI 10.1016/j.profoo.2011.09.265.
10. Zhang, C., Garrison, T. F., Madbouly, S. A., Kessler, M. R. (2017). Recent advances in vegetable oil-based polymers and their composites. *Progress in Polymer Science, 71,* 91–143. DOI 10.1016/j.progpolymsci.2016.12.009.
11. Liu, L., Lu, J., Zhang, Y., Liang, H., Liang, D. et al. (2019). Thermosetting polyurethanes prepared with the aid of a fully bio-based emulsifier with high bio-content, high solid content, and superior mechanical properties. *Green Chemistry, 21(3),* 526–537. DOI 10.1039/C8GC03560A.
12. Feng, Y., Liang, H., Yang, Z., Yuan, T., Luo, Y. et al. (2017). A solvent-free and scalable method to prepare soybean-oil-based polyols by thiol-ene photo-click reaction and biobased polyurethanes therefrom. *ACS Sustainable Chemistry & Engineering, 5(8),* 7365–7373. DOI 10.1021/acssuschemeng.7b01672.
13. Huang, J., Yuan, T., Ye, X., Man, L., Zhou, C. et al. (2018). Study on the UV curing behavior of tung oil: Mechanism, curing activity and film-forming property. *Industrial Crops and Products, 112,* 61–69. DOI 10.1016/j.indcrop.2017.10.061.
14. Liu, L., Liang, H., Zhang, J., Zhang, P., Xu, Q. et al. (2018). Poly (vinyl alcohol)/Chitosan composites: Physically transient materials for sustainable and transient bioelectronics. *Journal of Cleaner Production, 195,* 786–795. DOI 10.1016/j.jclepro.2018.05.216.
15. Jia, P., Zhang, M., Hu, L., Feng, G., Bo, C. et al. (2015). Synthesis and application of phosphaphenanthrene groups-containing soybean-oil-based plasticizer. *Industrial Crops and Products, 76,* 590–603. DOI 10.1016/j.indcrop.2015.07.034.
16. Jia, P. Y., Feng, G. D., Hu, Y., Zhou, Y. H. (2016). Synthesis and evaluation of a novel N-P-containing oil-based fire-retardant plasticizer for poly (vinyl chloride). *Turkish Journal of Chemistry, 40(1),* 65–75. DOI 10.3906/kim-1503-2.
17. Jia, P., Hu, L., Feng, G., Bo, C., Zhou, J. et al. (2017). Design and synthesis of a castor oil based plasticizer containing THEIC and diethyl phosphate groups for the preparation of flame-retardant PVC materials. *RSC Advances, 7(2),* 897–903. DOI 10.1039/C6RA25014A.
18. Jia, P., Hu, L., Zhang, M., Feng, G., Zhou, Y. (2017). Phosphorus containing castor oil based derivatives: Potential non-migratory flame retardant plasticizer. *European Polymer Journal, 87,* 209–220. DOI 10.1016/j.eurpolymj.2016.12.023.
19. Wang, X., Zhang, Y., Liang, H., Zhou, X., Fang, C. et al. (2019). Synthesis and properties of castor oil-based waterborne polyurethane/sodium alginate composites with tunable properties. *Carbohydrate Polymers, 208,* 391–397. DOI 10.1016/j.carbpol.2018.12.090.
20. Patil, D. K., Agrawal, D. S., Mahire, R. R., More, D. H. (2016). Synthesis, characterization and controlled release studies of ethyl cellulose microcapsules incorporating essential oil using an emulsion solvent evaporation method. *American Journal of Essential Oils and Natural Products, 4(1),* 23–31.
21. Nath, B., Nath, L. K., Mazumder, B., Kumar, P., Sharma, N. et al. (2010). Preparation and characterization of salbutamol sulphate loaded ethyl cellulose microspheres using water-in-oil-oil emulsion technique. *Iranian Journal of Pharmaceutical Research: IJPR, 9(2),* 97.
22. Aguiar, J., Costa, R., Rocha, F., Estevinho, B. N., Santos, L. (2017). Design of microparticles containing natural antioxidants: Preparation, characterization and controlled release studies. *Powder Technology, 313,* 287–292. DOI 10.1016/j.powtec.2017.03.013.
23. Lin, Y., Zhu, C., Alva, G., Fang, G. (2018). Microencapsulation and thermal properties of myristic acid with ethyl cellulose shell for thermal energy storage. *Applied Energy, 231,* 494–501. DOI 10.1016/j.apenergy.2018.09.154.
24. Lvov, Y., Wang, W., Zhang, L., Fakhrullin, R. (2016). Halloysite clay nanotubes for loading and sustained release of functional compounds. *Advanced Materials, 28(6),* 1227–1250. DOI 10.1002/adma.201502341.
25. Afrasiabi Garekani, H., Sanadgol, N., Dehghan Nayyeri, N., Nokhodchi, A., Sadeghi, F. (2018). Peculiar effect of polyethylene glycol in comparison with triethyl citrate or diethyl phthalate on properties of ethyl cellulose microcapsules containing propranolol hydrochloride in process of emulsion-solvent evaporation. *Drug Development and Industrial Pharmacy, 44(3),* 421–431. DOI 10.1080/03639045.2017.1395460.

26. Lin, G., Chen, H., Zhou, H., Zhou, X., Xu, H. (2018). Preparation of tea tree oil/poly(styrene-butyl methacrylate) microspheres with sustained release and anti-bacterial properties. *Materials, 11(5),* 710. DOI 10.3390/ma11050710.
27. Lee, D., Cohen, R. E., Rubner, M. F. (2005). Antibacterial properties of Ag nanoparticle loaded multilayers and formation of magnetically directed antibacterial microparticles. *Langmuir, 21(21),* 9651–9659. DOI 10.1021/la0513306.
28. Chen, H., Lin, Y., Xu, H., Cheng, D., Gong, S. et al. (2017). Preparation of sustained-release chlorpyrifos particles via the emulsification coacervation method and their sustained-release performance. *Journal of Macromolecular Science, Part A, 54(2),* 91–96. DOI 10.1080/10601325.2017.1261621.
29. Chen, H., Lin, G., Zhou, H., Zhou, X., Xu, H. et al. (2018). Preparation of Avermectin/Grafted CMC nanoparticles and their sustained release performance. *Journal of Polymers and the Environment, 26(7),* 2945–2953. DOI 10.1007/s10924-018-1182-y.
30. Mirabedini, S., Dutil, I., Farnood, R. (2012). Preparation and characterization of ethyl cellulose-based core–shell microcapsules containing plant oils. *Colloids and Surfaces A: Physicochemical and Engineering Aspects, 394,* 74–84. DOI 10.1016/j.colsurfa.2011.11.028.
31. Haghi, H., Mirabedini, S., Imani, M., Farnood, R. (2014). Preparation and characterization of pre-silane modified ethyl cellulose-based microcapsules containing linseed oil. *Colloids and Surfaces A: Physicochemical and Engineering Aspects, 447,* 71–80. DOI 10.1016/j.colsurfa.2014.01.021.
32. Higuchi, T. (1963). Mechanism of sustained-action medication. Theoretical analysis of rate of release of solid drugs dispersed in solid matrices. *Journal of Pharmaceutical Sciences, 52(12),* 1145–1149. DOI 10.1002/jps.2600521210.
33. Korsmeyer, R. W., Gurny, R., Doelker, E., Buri, P., Peppas, N. A. (1983). Mechanisms of solute release from porous hydrophilic polymers. *International Journal of Pharmaceutics, 15(1),* 25–35. DOI 10.1016/0378-5173(83)90064-9.
34. Liang, H., Liu, L., Lu, J., Chen, M., Zhang, C. (2018). Castor oil-based cationic waterborne polyurethane dispersions: Storage stability, thermo-physical properties and antibacterial properties. *Industrial Crops and Products, 117(1),* 169–178. DOI 10.1016/j.indcrop.2018.02.084.
35. Wang, X., Liang, H., Jiang, J., Wang, Q., Luo, Y. et al. (2020). A cysteine derivative-enabled ultrafast thiol–ene reaction for scalable synthesis of a fully bio-based internal emulsifier for high-toughness waterborne polyurethanes. *Green Chemistry, 22(1),* 5722–5729. DOI 10.1039/D0GC02213F.
36. Zhang, Y., Liu, B., Huang, K., Wang, S., Quirino, R. et al. (2020). Eco-Friendly castor oil-based delivery system with sustained pesticide release and enhanced retention. *ACS Applied Materials & Interfaces, 12(33),* 37607–37618. DOI 10.1021/acsami.0c10620.
37. Liu, L., Lu, J., Zhang, Y., Liang, H., Liang, D. et al. (2019). Thermosetting polyurethanes prepared with the aid of a fully bio-based emulsifier with high bio-content, high solid content, and superior mechanical properties. *Green Chemistry, 3(21),* 526–537. DOI 10.1039/C8GC03560A.
38. Klemm, D., Cranston, E., Fischer, D., Gama, M., Kedzior, S. et al. (2018). Nanocellulose as a natural source for groundbreaking applications in materials science: Today's state. *Materialstoday, 21(7),* 720–748.
39. Tan, T., Lee, H., Dabdawb, W. A. Y., Hamid, S. B. B. (2018). A review of nanocellulose in the drug-delivery system. *Materials for Biomedical System, 5(1),* 131–164.
40. Lin, N., Dufresne, A. (2014). Nanocellulose in biomedicine: Current status and future prospect. *European Polymer Journal, 59(1),* 302–325. DOI 10.1016/j.eurpolymj.2014.07.025.
41. Sharma, P., Chattopadhyay, A., Sharma, S., Hsiao, B. (2017). Efficient removal of UO_2^{2+} from water using carboxycellulose nanofibers prepared by the nitro-oxidation method. *Industrial & Engineering Chemistry Research, 56(46),* 13885–13893. DOI 10.1021/acs.iecr.7b03659.
42. Sharma, P., Chattopadhyay, A., Sharma, S., Geng, L., Amiralian, N. et al. (2018). Nanocellulose from spinifex as an effective adsorbent to remove cadmium(II) from water. *ACS Sustainable Chemistry & Engineering, 6(3),* 3279–3290. DOI 10.1021/acssuschemeng.7b03473.

43. Sharma, P., Sharma, S., Lindstrom, T., Hsiao, B. (2020). Nanocellulose-enabled membranes for water purification: Perspectives. *Advanced Sustainable Systems, 4(5),* 190014.
44. Sharma, S., Sharma, P., Lin, S., Zhan, C., Hsiao, B. (2020). Reinforcement of natural rubber latex using jute carboxycellulose nanofibers extracted using nitro-oxidation method. *Nanomaterial, 10(4),* 706. DOI 10.3390/nano10040706.
45. Sharma, P., Chattopadhyay, A., Zhan, C., Geng, L., Hsiao, B. (2018). Lead removal from water using carboxycellulose nanofibers prepared by nitro-oxidation method. *Cellulose, 25(3),* 1961–1973. DOI 10.1007/s10570-018-1659-9.